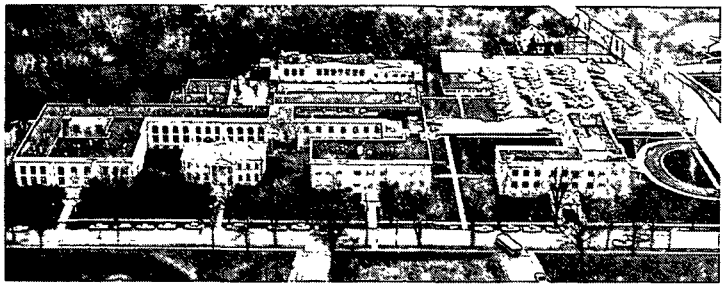

THE INSTITUTE OF PAPER CHEMISTRY, APPLETON, WISCONSIN

IPC TECHNICAL PAPER SERIES
NUMBER 225

EFFECTS OF PHYSICAL STRUCTURE ON THE ALKALINE DEGRADATION OF HYDROCELLULOSE

VICTOR M. GENTILE, LELAND R. SCHROEDER, AND RAJAI H. ATALLA

FEBRUARY, 1987

Effects of Physical Structure on the Alkaline Degradation of Hydrocellulose

Victor M. Gentile, Leland R. Schroeder, and Rajai H. Atalla

Portions of this work were used by VMG as partial fulfillment of the requirements for the Doctor of Philosophy degree at The Institute of Paper Chemistry. This manuscript has been submitted for inclusion in the Symposium on Solid State Characterization of Cellulose, R. H. Atalla, Editor, to be published in the ACS Symposium Series

Effects of Physical Structure on the Alkaline Degradation of Hydrocellulose

Victor M. Gentile, Leland R. Schroeder, and Rajai H. Atalla

The Institute of Paper Chemistry
Appleton, Wisconsin 54912

Degradations of fibrous cotton hydrocellulose and an amorphous hydrocellulose were conducted in oxygen-free 1.0M NaOH at 60 and 80°C. The physical structure of the fibrous hydrocellulose was not significantly altered, while the amorphous hydrocellulose underwent partial recrystallization into the cellulose II form and some loss of amorphous material through degradation. Endwise depolymerization (peeling) and formation of stable carboxylic acid endgroups (chemical stopping) were more rapid and extensive with the amorphous substrate. Both peeling and chemical stopping were inhibited by the more highly ordered physical structure of the fibrous hydrocellulose and the majority of degrading molecules terminated to stable inaccessible reducing endgroups, that is, by physical stopping. In contrast, chemical stopping was the dominant stabilization mechanism in the amorphous hydrocellulose. The rate of chemical stopping relative to peeling increased with temperature for both substrates. In addition, random chain cleavage, normally believed to be important only at much higher temperatures, was detected in the amorphous hydrocellulose.

Alkaline degradation of cellulose occurs by random cleavage of glycosidic linkages and by stepwise elimination of monomer units from the reducing end (peeling) (1,2). These reactions occur in competition with another reaction which stabilizes cellulose against alkaline degradation by converting the reducing endgroup to an alkali-stable, carboxylic acid endgroup (chemical stopping).

Though the major alkaline reactions of cellulose have been relatively well defined, the role of cellulose physical structure in those reactions has not been clearly established. Cellulose molecules have been reported to undergo physical stopping of the peeling reaction when a molecule is peeled back to a crystalline region in the cellulose structure, with the result that the reducing endgroup

becomes inaccessible to the alkaline medium (3-5). It is also reported that for native cellulose the rate of peeling relative to chemical stopping is higher than for mercerized cellulose (3,6-8). Furthermore, random chain cleavage occurs more rapidly in mercerized cellulose than in native cellulose (6). These findings suggest that both molecular accessibility and conformation (i.e., cellulose I or II) influence the susceptibility of cellulose molecules to alkaline reactions. However, separating the different effects of physical structure from the inherent reactivity of the cellulose molecule (in an alkaline environment) is made difficult by its limited solubility in alkaline solutions.

In the present study, the role of cellulose physical structure in alkaline reactions was investigated by comparing the alkaline degradation of highly crystalline (cellulose I) fibrous hydrocellulose with that of amorphous (noncrystalline) hydrocellulose. The amorphous substrate was taken as a cellulose model the reactivity of which would most closely approximate that of alkali-soluble cellulose. The availablity of such an approximation to the inherent reactivity of cellulose allowed evaluation of the effects of the more highly ordered structure of the fibrous hydrocellulose.

Results and Discussion

Experimental Approach. The experimental study was a comparison of the alkaline degradations of fibrous and amorphous hydrocelluloses in oxygen-free 1.0M NaOH, at 60 and 80°C. The fibrous hydrocellulose was predominantly crystalline (cellulose I) and therefore served as a substrate which would undergo alkaline reactions with significant physical structure effects. In contrast, the amorphous hydrocellulose was noncrystalline (9,10). Thus, it was a substrate which would experience substantially less structural constraint during its alkaline reactions.

The fibrous hydrocellulose was prepared by mild acid hydrolysis of cotton fibers to provide sufficient numbers of reducing endgroups for peeling and stopping to occur at measurable rates. The amorphous hydrocellulose was prepared by dissolving the fibrous hydrocellulose in the dimethylsulfoxide-paraform-aldehyde (DMSO-PF) solvent (9-12) and then regenerating the hydrocellulose with a sodium methoxide-isopropoxide solution (9,10). Both hydrocelluloses were freeze-dried during preparation and after degradation to minimize drying-induced structural changes. Thus, structural changes caused by the alkaline medium and the degradation reactions could be detected more readily.

Data on endgroup contents and number-average degrees of polymerization ($\overline{DP}_n$) for the hydrocellulose substrates are presented in Table I. The hydrocelluloses have similar numbers of carboxylic acid endgroups formed during purification of the cotton fibers. But only the amorphous hydrocellulose contained no inaccessible reducing endgroups, demonstrating the capacity of the dissolution/regeneration process to enhance accessibility (9,10). On the other hand, the total reducing endgroup content of the amorphous hydrocellulose was greater than that of the fibrous hydrocellulose. This, together with the lower $\overline{DP}_n$ of the amorphous substrate, indicates that some chain cleavage occurred during regeneration. The chain cleavage was

apparently related to the scale-up of the process, since no cleavage was detected when relatively small samples (< 2 g) were regenerated (9). For this reason, in comparisons of the peeling and stopping reactions of the two substrates, reaction rates were corrected for the different accessible (reactive) reducing endgroup contents.

Table I. Endgroup[a] and $\overline{DP_n}$[b] Data for Hydrocellulose Substrates

	Fibrous Hydrocellulose	Amorphous Hydrocellulose
Carboxylic acid endgroups	1.09×10^{-3}	1.02×10^{-3}
Accessible reducing endgroups	1.13×10^{-3}	3.42×10^{-3}
Inaccessible reducing endgroups	0.15×10^{-3}	0
Total reducing endgroups	1.28×10^{-3}	3.42×10^{-3}
$\overline{DP_n}$	422	225

[a]Endgroup values expressed as mole fractions of total monomer units.
[b]Calculated from the total endgroups content^{-1}.

During the course of the alkaline degradations, both physical and chemical structures of the hydrocelluloses were monitored. Hydroxyl accessibility (13) was determined as a practical measure of the fraction of molecules accessible to the alkaline medium. The crystalline structure was characterized by x-ray diffraction (14). In addition, Raman (15) and solid-state carbon-13 nuclear magnetic resonance (^{13}C-NMR) (16,17) spectra were utilized to assess conformational changes. Yield loss was determined gravimetrically and taken as a measure of anhydroglucose units lost due to peeling. The chemical stopping reaction was monitored by measuring carboxylic acid endgroup formation, using methylene blue absorption values (10). The reactive species for both peeling and stopping, that is, the accessible reducing endgroups, were detected by selective reduction with tritium-labeled sodium borohydride (9,10). Inaccessible (nonreactive) reducing endgroups were also detected by reduction with sodium borohydride-^{3}H after they were made accessible via the previously discussed regeneration technique (9). It was therefore possible to detect the so-called "physical stopping" of the peeling reaction as evidenced in the formation of inaccessible or unreactive reducing endgroups.

The physical structure data together with the alkaline reaction data permitted evaluation of the effects of physical structure on alkaline degradation of cellulose.

Alkaline Degradations - Change in Physical Structure. The hydroxyl accessibility of the fibrous hydrocellulose was initially 51.4 ± 0.8%. In contrast, the amorphous substrate had an accessibility of 99.2 ± 1.0%. Exposure of the fibrous hydrocellulose to the alkaline media caused the accessibility to decrease slightly to 50.7 ± 1.0% and 49.1 ± 1.2% at 60 and 80°C, respectively, but accessibility did not change significantly during the reaction periods (0-168 hr).

The accessibility of the amorphous hydrocellulose, however, did decline, both upon exposure to the alkaline media and during the reaction periods (Figure 1). This indicates both recrystallization and selective removal of amorphous material.

X-ray diffractograms of the fibrous hydrocellulose (Figure 2) exhibit the characteristic 002, 101, and $10\bar{1}$ reflections of the cellulose I crystalline lattice (14,18). The sharply defined peaks indicate a high degree of crystallinity. Although there appears to be a slight increase in peak intensity in the diffractogram of the zero-time sample relative to that of the initial substrate, no further change is evident in the diffractogram of the 48-hour sample. Thus, x-ray diffraction confirms that the fibrous hydrocellulose does not undergo significant change in physical structure during degradation.

The diffuse diffractogram of the initial amorphous substrate (Figure 3) is indicative of noncrystalline cellulose (19). The diffractogram of the zero-time sample exhibits a set of weak reflections corresponding to the 002, 101, and $10\bar{1}$ planes of the cellulose II crystalline lattice (14,18). The poorly defined peaks indicate a relatively low degree of crystallinity. Since the diffractogram of the 48-hour sample displays slightly more intense reflections, a small increase in the cellulose II content occurred during the reaction period. This is consistent with the hydroxyl accessibility data.

Raman spectra of the fibrous hydrocellulose in the conformation sensitive 250 to 650 cm^{-1} region have relatively intense cellulose I bands (Figure 4), indicating that the molecules are predominantly in the cellulose I conformation (15). This is best demonstrated by the intense band at 378 cm^{-1}. The lack of sigificant differences in the spectra of the initial substrate, zero-time sample, and 48-hour sample confirm that no significant changes in physical structure occurred during degradation.

In contrast, the same region in the Raman spectrum of the initial amorphous substrate exhibits broad bands (Figure 5) indicative of irregular sequences of conformations along the cellulose chains (15). The emergence of a band at 355 cm^{-1} in the spectrum of the zero-time sample indicates the presence of the cellulose II allomorph. The additional, small increase in band intensity in the spectrum of the 48-hour sample again demonstrates a further slight increase in cellulose II content during degradation.

The solid-state ^{13}C-NMR spectra of the fibrous hydrocellulose also demonstrate the predominance of the cellulose I allomorph (Figure 6). All three spectra contain the sharp resonances associated with the cellulose I conformation and the broader C-4 and C-6 resonances indicative of regions of three-dimensional disorder and crystallite surfaces (16,17). The relative intensities of the sharp and broad resonances of the three spectra are similar, again demonstrating the lack of change in physical structure during degradation.

In comparison, the ^{13}C-NMR spectrum of the initial amorphous subsrate exhibits only broad resonances (Figure 7) characteristic of regions of three-dimensional disorder (16,17). The progressive appearance of sharper resonances in the spectra of the zero-time and 48-hour samples indicates increasing conformational order.

Resonance locations and multiplicities are characteristic of the cellulose II allomorph, confirming the results of x-ray diffraction and Raman spectroscopy.

The absence of change in the physical structure of the fibrous hydrocellulose during degradation suggests three alternative hypotheses. First, selective degradation of amorphous cellulose could have occurred but to an extent not detectable by the methods applied. Second, removal of amorphous material could have been accompanied by a comparable amount of decrystallization of cellulose I domains. Finally, cellulose removed during degradation may have displayed partial cellulose I character. This would involve molecules in slightly distorted cellulose I domains (tilted or twisted segments of elementary fibril) and at crystallite surfaces (20), since removal of either would not result in detectable changes in physical structure. Alkaline reaction data presented in the following section tend to support the latter hypothesis.

The increase in cellulose II character and decrease in accessibility of the amorphous hydrocellulose upon exposure to the alkaline medium and during the reaction interval definitely indicate partial recrystallization. However, selective removal of amorphous cellulose may have occurred simultaneously. This additional possibility is consistent with the alkaline reaction data.

Peeling and Stopping Reactions. The yield loss during alkaline degradation was more rapid and extensive for the amorphous hydrocellulose than for the fibrous hydrocellulose, at both 60 and 80°C (Figure 8). However, the evolution of yield loss with time was different at 60 and 80°C. While at 60°C yield loss occurred throughout the time interval studied (168 hr), the yield of both substrates leveled off after ca. 48 hours at 80°C. While small amounts of pectic material are probably lost during the degradations, such losses are insignificant relative to yield losses due to peeling (10).

Direct comparison of yield data for the two substrates is not possible due to the differences in initial accessible reducing endgroup contents (Table I). The kinetic model used by Haas, et al. (5) was therefore employed to provide a basis for comparison of reaction rates of molecules within the two substrates. This model incorporates pseudo-first-order rate expressions for peeling (Equation 1), chemical stopping (Equation 2), and physical stopping (Equation 4); our notation differs from that of Haas, et al. In all three rate expressions, the reaction rates are related to the number of accessible reducing endgroups by pseudo-first-order rate coefficients. Thus, the rate coefficients reflect the reactivities of accessible reducing endgroups occupying different structural environments.

Since the yield losses were predominantly due to peeling (10), the pseudo-first-order rate expression for peeling can be written:

$$d[Y_1]/dt = k_p[ARE_t] \qquad (1)$$

where $[Y_1]$ = Yield loss, as mole fraction of total monomer units at zero-time

t = Time, hr
k_p = Rate coefficient for peeling, hr^{-1}
$[ARE_t]$ = Accessible reducing endgroup content at time "t," as mole fraction of total monomer units at zero-time

The derivative in Equation 1 was evaluated at selected reaction times from the slopes of plots of yield loss versus reaction time. Values of k_p, calculated from Equation 1, are listed in Table II.

Table II. Rate Coefficients for Peeling[a]

Reaction Time, hr	60°C		80°C	
	Fibrous	Amorphous	Fibrous	Amorphous
0	4.13	6.16	27.9	40.4
2	3.28	5.52	8.91	13.6
4	2.74	4.16	8.06	6.23
48	0.48	0.60	1.38	0.19
96	0.38	0.53	0.60	0.14

[a] k_p, hr^{-1}.

In all cases, k_p decreased with reaction time. Thus, the accessible reducing endgroups in both hydrocelluloses were more reactive initially, apparently due to their location in less ordered regions of the respective physical structures. As the less ordered material was removed, the accessible reducing endgroups occupied increasingly ordered regions of the structures and were therefore less reactive.

The higher k_p values for the amorphous hydrocellulose throughout the 60°C reaction and during the initial period of the 80°C reaction indicate that the accessible reducing endgroups were more reactive than those in the fibrous hydrocellulose. This coincides with the periods during which the accessibility decreased (Figure 1), suggesting that selective removal (peeling) of amorphous material did occur. Thus, the less ordered environment occupied by the degrading molecules in the amorphous hydrocellulose clearly rendered them more susceptible to peeling.

During the later period of the 80°C reaction, the amorphous hydrocellulose exhibited a lower value of k_p than the fibrous hydrocellulose. Since this corresponds to the period during which the hydroxyl accessibility of the amorphous hydrocellulose leveled-off (Figure 1), it appears that the population of degradable chains with accessible reducing endgroups had been depleted. Consequently, peeling was probably occurring close to cellulose II domains where it was significantly inhibited. In contrast, peeling progressed more slowly toward the cellulose I domains of the fibrous hydrocellulose, for example, in slightly distorted cellulose I domains, but was also strongly inhibited at the faces of more perfect cellulose I crystallites. The degree of inhibition of peeling is evidenced by the convergence of 60 and 80°C k_p values for both substrates at longer reaction times.

In the case of chemical stopping, the rate of formation of carboxylic acid endgroups is also proportional to the number of accessible reducing endgroups. The pseudo-first-order rate expression is given by:

$$[AE]/dt = k_{cs}[ARE_t] \quad (2)$$

where [AE] = Carboxylic acid endgroup content, as mole fraction of total monomer units at zero-time
k_{cs} = Rate coefficient for chemical stopping, hr^{-1}

Carboxylic acid endgroup contents were first corrected for losses of carboxylic acid groups associated with pectic material lost during the reactions (10). Values of k_{cs} were then determined at specific time intervals by the same graphical procedure as outlined for k_p; the values of k_{cs} are given in Table III.

Table III. Rate Coefficients for Chemical Stopping[a]

Reaction time, hr	60°C		80°C	
	Fibrous	Amorphous	Fibrous	Amorphous
0	0.0142	0.0302	0.106	0.262
2	0.0112	0.0271	0.0338	0.107
4	0.0094	0.0204	0.0305	0.0808
48	0.0015	0.0057	0.0119	0.0225
96	0.0010	0.0055	0.0073	0.0205

[a] k_{cs}, hr^{-1}.

The rate coefficients for chemical stopping decreased with time for both substrates in a pattern similar to that for peeling. Thus, as the accessible reducing endgroups occupied progressively more ordered regions of the structures, their reactivity toward chemical stopping also decreased.

The amorphous hydrocellulose exhibited higher values of k_{cs} throughout both the 60 and 80°C reactions. During the early period of the 80°C reaction and throughout the 60°C reaction, when the rate coefficient for peeling was higher for the amorphous substrate (Table II), its higher k_{cs} value can be primarily attributed to the reaction occurring in less ordered regions of the structure. However, this could not account for the behavior in the later period of the 80°C reactions, where peeling was apparently hindered to similar extents by the crystalline regions of both structures. Therefore, it is concluded that the cellulose II domains in the amorphous substrate did not inhibit chemical stopping as drastically as the cellulose I domains in the fibrous substrate.

Further clarification of these differences is provided by comparing the relative rates of peeling and chemical stopping for the two substrates. Average values of k_p/k_{cs} (Table IV) were calculated using Equation 3, derived by dividing Equation 1 by Equation 2.

$$d[Y_1]/d[AE] = k_p/k_{cs} \quad (3)$$

The relative rates of peeling and chemical stopping were higher for the fibrous hydrocellulose throughout the reactions. For the amorphous substrate, the values of k_p/k_{cs} were lower at the outset, and decreased substantially, at longer reaction times. Since k_p/k_{cs} remained constant throughout the fibrous hydrocellulose reactions, the relative reactivity of its accessible reducing endgroups toward both reactions appears not to change as the reactions progress from regions of lower order to regions of higher order. This is consistent with the less ordered regions exhibiting some cellulose I character; reference here is to slightly distorted cellulose I domains and crystallite surfaces (20). In the later periods of the amorphous hydrocellulose reactions, however, peeling was inhibited much more than chemical stopping. This is consistent with the earlier proposal that cellulose II domains do not hinder chemical stopping as effectively as cellulose I domains, while both crystalline forms are highly resistant to peeling. Thus, the physical presence of the crystalline domains appears to deter the progression of peeling along a cellulose molecule, while both the degree of structural order and the particular molecular conformation dictate the reactivity of an accessible reducing endgroup toward chemical stopping.

Table IV. Relative Rates of Peeling and Chemical Stopping

Reaction	k_p/k_{cs}
Fibrous 60°C (0-168 hr)	291
Fibrous 80°C (0-96 hr)	264
Amorphous 60°C (0-48 hr)	204
(48-168 hr)	84
Amorphous 80°C (0-4 hr)	154
(4-96 hr)	23

These findings are consistent with results of comparative alkaline degradation studies of native (cellulose I) and mercerized (cellulose II) cellulose (3,6-8). In addition, decreases in k_p/k_{cs} for both substrates with increasing temperature are in agreement with the higher activation energy reported for chemical stopping versus peeling in hydrocellulose (5).

In addition to undergoing chemical stopping reactions, cellulose molecules also are thought to terminate in reducing endgroups which are physically incapable of reacting due to their inaccessbility to the alkaline medium (3-5). The term "physical stopping" has been used to characterize the formation of inaccessible reducing endgroups (nonreactive) on molecules which previously contained accessible (reactive) reducing endgroups. The pseudo-first-order rate expression for physical stopping is written:

$$d[IRE]/dt = k_{ps}[ARE_t] \quad (4)$$

where [IRE] = Inaccessible reducing endgroup content, as mole fraction of total monomer units at zero-time

k_{ps} = Psudo-first-order rate coefficient for physical stopping

Although physical stopping is not a chemical reaction, per se, k_{ps} values determined using Equation 4 may be compared to k_{cs} values, providing a measure of the relative importance of the two modes of stopping. Furthermore, comparison of k_{ps} values for two substrates gives an indication of the relative extent of structural hindrance to peeling.

In both the 60 and 80°C reactions, the fibrous hydrocellulose exhibited higher k_{ps} values than the amorphous hydrocellulose (Table V). This appears to be due to the involvement of more molecules in crystalline domains of the fibrous substrate. The greater inhibition of chemical stopping by cellulose I than cellulose II domains may also have contributed to this effect by allowing more molecules in the fibrous hydrocellulose to peel to a point where the reducing endgroup would be inaccessible.

Table V. Rate Coefficients for Physical Stopping[a]

Reaction Time, hr	60°C		80°C	
	Fibrous	Amorphous	Fibrous	Amorphous
0	0.0410	0.0142	0.363	0.154
2	0.0218	0.0137	0.0812	0.0700
4	0.0157	0.0132	0.0543	0.0195
48	0.0032	0.0021	0	0
96	0.0028	0.0019	0	0

[a] k_{ps}, hr^{-1}.

At 80°C and for longer reaction times, both hydrocelluloses ceased physical stopping. This may be an indication that each physical structure has some maximum number of potential physical stopping sites. As a consequence, inaccessible reducing endgroups could become accessible as adjacent molecules are removed by peeling, giving rise to a steady state distribution of accessible and inacessible reducing endgroups.

Except for the later period of the 80°C reactions, the fibrous hydrocellulose exhibited a higher value of k_{ps} (Table V) than k_{cs} (Table IV). Consequently the degradation of a majority of the molecules in the fibrous hydrocellulose was terminated by physical rather than chemical stopping processes. In contrast, chemical stopping was the dominant mechanism of stabilization in the amorphous hydrocellulose.

Random Chain Cleavage Reaction. In addition to peeling, cellulose is also reported to undergo random cleavage of glycosidic linkages in alkaline media (1,2). This reaction results in the formation of

one reducing and one nonreducing endgroup. Since reducing endgroups can also be involved in peeling and stopping reactions, it is not possible to monitor directly their formation due to random chain cleavage. However, the rate of chain cleavage can be characterized by monitoring increases in the total number of endgroups. Accurate characterization of the reaction does require that no other changes in the total number of endgroups occur, as for example, from loss of molecules by complete peeling or dissolution.

During degradation of the fibrous hydrocellulose, no changes in total endgroup content were detected (Table VI). This is consistent with results of previous studies (6,7) in which chain cleavage was found to be important in native cellulose only above 100°C.

Table VI. Total Endgroup Contents[a] of Hydrocelluloses

Reaction Time, hr	60°C		80°C	
	Fibrous	Amorphous	Fibrous	Amorphous
0	1.94	4.13	1.88	4.51
2	1.94	3.57	1.90	4.28
4	1.92	3.44	1.96	4.35
8	2.04	3.52	1.96	4.44
24	1.95	3.59	1.89	4.96
48	1.92	3.65	1.89	5.05
96	1.86	3.76	1.90	5.35
168	1.89	4.09	--	--

[a]Expressed as 10^3 x mole fraction of total monomer units at zero-time.

In contrast, the amorphous hydrocellulose underwent initial decline in total endgroup content (Table VI) which may be attributed to complete peeling and/or dissolution of low DP molecules. After the initial periods, total endgroup contents increased gradually at both 60 and 80°C, indicating that random chain cleavage occurred. Random chain cleavage must also have occurred during the initial periods but was probably masked by the more substantial negative effects of complete peeling or dissolution on the total endgroup contents.

The amorphous substrate suffered the most rapid decline in hydroxyl accessibility (Figure 1) during the same periods in which total endgroup losses occurred. This indicates that complete peeling or dissolution primarily involved molecules existing entirely within amorphous regions and became insignificant once the majority of highly accessible chains had been removed or chemically stabilized. Further support is thus provided for the hypothesis that selective peeling of amorphous material contributes to the higher rate coefficient of peeling in the case of the amorphous hydrocellulose (Table II). The comparative lack of similar losses from the fibrous substrate suggests that the large majority of molecules were embedded to some extent in crystalline regions.

Because endgroup losses occurred simultaneously with random chain cleavage during the initial periods, analysis of the total endgroup data for kinetics of chain cleavage was confined to the later reaction periods. Since the total number of monomer units, or yield, is essentially equal to the number of glycosidic linkages, the pseudo-first-order rate expression for random chain cleavage can be written as:

$$d[TE]/dt = k_{cc}[Y_t] \quad (5)$$

where [TE] = Total endgroup content, as mole fraction of total monomer units at zero-time
k_{cc} = Rate coefficient for random chain cleavage, hr^{-1}
$[Y_t]$ = Yield, as mole fraction of total monomer units at time "t"

Rate coefficients for random chain cleavage in the 60°C amorphous hydrocellulose reaction decreased gradually from 8 to 168 hours (Table VII). At 80°C, the decrease in k_{cc} occurred more rapidly between 2 and 48 hours, with a more gradual decline up to 96 hours. This reflects the more rapid decline in accessibility of the amorphous hydrocellulose at 80°C (Figure 1). Thus, random chain cleavage appears to be inhibited by the larger cellulose II fraction that formed in the amorphous substrate at 80°C.

Table VII. Rate Coefficients[a] for Random Chain Cleavage

Reaction Time, hr	60°C		80°C	
	Fibrous	Amorphous	Fibrous	Amorphous
0	0	ND	0	ND
2	0	ND	0	5.78×10^{-5}
8	0	8.42×10^{-6}	0	5.31×10^{-5}
48	0	8.38×10^{-6}	0	0.82×10^{-5}
96	0	8.34×10^{-6}	0	0.49×10^{-5}
168	0	7.53×10^{-6}	--	--

[a] k_{cc}, hr^{-1}.
ND = Rate coefficients not determined due to simultaneous complete peeling or dissolution

The absence of chain cleavage in the fibrous hydrocellulose suggests that its disordered regions were more highly structured than the corresponding regions of the amorphous hydrocellulose. This is consistent with the results of a previous study (6) in which mercerized cellulose was found to be more susceptible to random chain cleavage than native cellulose. Another implication is that the disordered regions associated with the two crystalline polymorphs display different degrees of structural order, giving rise to differences in reactivity. Thus, in addition to molecular mobility and accessibility, the particular molecular conformation

appears to influence susceptibility to the random chain cleavage reaction.

Conclusions

Alkaline peeling and chemical stopping occur more rapidly in the amorphous regions of amorphous hydrocellulose than in the disordered regions of fibrous hydrocellulose. In addition, random chain cleavage at 60 and 80°C occurs only in amorphous hydrocellulose. Therefore, it is proposed that the disordered regions of the fibrous hydrocelluose consist of less reactive molecules at crystallite surfaces and in slightly distorted crystalline domains, as previously suggested (20).

Peeling is inhibited to similar extents by the crystalline order of both cellulose I and II allomorphs, while chemical stopping is significantly more inhibited in the cellulose I allomorph. This is consistent with the higher ratio of the rate of chemical stopping to that of peeling typically reported for mercerized cellulose in comparison to native cellulose (3,6-8).

Physical stopping, that is, formation of inaccessible reducing endgroups, occurs when peeling of molecular chains reaches the crystalline domains in both cellulose I and II. The relative rates of physical and chemical stopping are dictated by the number of molecules involved in crystalline domains. In a previous study (5), cellulose molecules were reported to maintain constant reactivity toward peeling and chemical stopping unless physical stopping occurred. However, the results of the present study indicate that reactivity diminishes gradually as reactions approach more highly ordered regions of physical structure. Simultaneously, abrupt physical stopping can occur.

The rate of chemical stopping increases with temperature relative to peeling in both fibrous and amorphous hydrocellulose. This observation is consistent with previous findings (5).

Experimental

Cellulose Substrates. Raw cotton fiber cut in ca. 0.25 inch lengths was purified by extraction with chloroform, 95% ethanol, boiling 1% (w/w) sodium hydroxide (oxygenfree), and diethylene triaminepentaacetic acid (0.15% w/v, pH 9) (10). Fibrous hydrocellulose was prepared by treating the purified fibers (60 g) with 0.1M hydrochloric acid (6L) at 40°C for 20 hours, washing with distilled water (until neutral), and then freeze-drying. Amorphous hydrocellulose was prepared by dropwise addition of a DMSO-PF solution of the fibrous hydrocellulose (0.2%, w/v, cellulose/DMSO, 3.5L) to 0.2M sodium methoxide-isopropoxide solution (1:1, v/v, methanol:isopropanol, 14L) (9,10). The resulting precipitate was washed with 0.2M sodium methoxide-isopropoxide, methanol (until neutral), 0.1M hydrochloric acid, and distilled water (until neutral), and then freeze-dried. Both the fibrous and amorphous hydrocelluloses were further dried in vacuo over phosphorus pentoxide to constant weight.

Degradation Procedure. Alkaline degradations were conducted in 316 stainless steel laboratory digesters (10). Hydrocellulose substrate

(400 mg) and oxygen-free 1.0M sodium hydroxide (40 mL) were sealed in the reaction vessels under nitrogen, and the vessels were rotated end-over-end at ca. 3 rpm in a constant temperature oil bath. The reaction mixtures were maintained at 60 or 80°C for the specified time interval, cooled to 20°C, and neutralized with 1.0M hydrochloric acid. Zero-time samples were prepared by limiting the time at the reaction temperature to ca. one minute. Degraded hydrocellulose was washed with 0.1M hydrochloric acid and distilled water (until neutral), and then freeze-dried. Yield was determined after further drying in vacuo over phosphorus pentoxide to constant weight.

Analytical Methods. Carboxylic acid endgroup contents were determined by methylene blue absorption using TAPPI Standard Method T237 su-63 with minor modifications (10). Accessible reducing endgroups were detected by reduction with sodium borohydride-^{3}H, and total reducing endgroups were determined similarly after regenerating the cellulose from the DMSO-PF solvent (9,10). Inaccessible reducing endgroup contents were calculated as total less accessible reducing endgroup contents.

Cellulose hydroxyl accessibility was measured by the deuteration method of Rouselle and Nelson (13), but the deuteration time (in liquid D_2O) was extended to 12 hours (10). X-ray diffractograms were collected on a Norelco diffractometer, using nickel-filtered, CuKα radiation. Raman spectra were acquired with a Jobin Yvon Ramanor Spectrometer, utilizing the 5145 Å line of an argon laser operated, at 100 mw, as the exciting source. Solid-state ^{13}C-NMR spectra were obtained on a General Electric S-100 instrument employing the combined techniques (16,17) of proton-carbon cross polarization, high power proton decoupling, and magic-angle sample spinning.

Acknowledgments

The authors wish to thank Dr. T. Early of GE-NMR Instruments Company, Inc. for obtaining the solid-state ^{13}C-NMR spectra and Mr. C. Woitkovich for acquiring the Raman spectra. V. M. Gentile sincerely appreciates fellowship support from The Institute of Paper Chemistry during this work.

References

1. Meller, A. Holzforschung 1960, 14, 78 and references cited therein.
2. Richards, G. N. In Cellulose and Cellulose Derivatives; Part V, p. 1007 and references cited therein, N. Bikales and L. Segal (Eds.), Wiley-Interscience, New York, 1971.
3. Machell, G.; Richards, G. N. Tappi 1958, 41, 12.
4. Colbran, R. L.; Davidson, G. F. J. Textile Inst. 1961, 52, T73.
5. Haas, D. W.; Hrutfiord, B. F.; Sarkanen, K. V. Appl. Polymer Sci. 1967, 11, 587.
6. Lai, Y.-Z.; Sarkanen, K. V. Cellulose Chem. Technol. 1967, 1, 517.

7. Franzon, O.; Samuelson, O. Svensk Papperstid. 1957, 60, 872.
8. Christofferson, K.; Samuelson, O. Svensk Papperstid. 1962, 65, 571.
9. Gentile, V. M.; Schroeder, L. R.; Atalla, R. H. J. Wood Chem. 1986, 6, 1.
10. Gentile, V. M. Doctoral Dissertation, The Institute of Paper Chemistry, Appleton, Wisconsin (1986).
11. Nicholson, M. D.; Johnson, D. C.; Haigh, F. C. Appl. Polymer Symp. 1976, 28, 931.
12. Baker, T. J.; Schroeder, L. R.; Johnson, D. C. Cellulose Chem. Technol. 1981, 15, 311.
13. Rouselle M. A.; Nelson, M. L. Textile Res. J. 1971, 41, 599.
14. Wadsworth, L.C.; Cuculo, L. C. In Modified Cellulosics, Part III, p. 117, R. M. Rowell and R. A. Young (Eds.), Academic Press, New York, 1978.
15. Atalla, R. H. J. Appl. Polymer Sci. (Appl. Polymer Symp.) 1983, 37, 295.
16. Earl, W. L.; VanderHart, D. L. Macromolecules 1981, 14, 570.
17. VanderHart, D. L.; Atalla, R. H. Macromolecules 1984, 17, 1465.
18. Tripp, V. M. In Cellulose and Cellulose Derivatives, Part IV, p. 305, N. Bikales and L. Segal (Eds.), Wiley-Interscience, New York, 1981.
19. Howsmon, J. A.; Sisson, W. A. In Cellulose, Part I, 2nd Ed., p. 231, E. Ott and H. M. Spurlin (Eds.), Interscience Publishers, New York, 1954.
20. Rowland, S. P. In Modified Cellulosics, Part III, p. 162, and references cited therein, R. M. Rowell and R. A. Young (Eds.), Academic Press, New York, 1978.

Figure 1. Hydroxyl accessibility of the amorphous hydrocellulose during degradation in 1.0M NaOH.

Figure 2. X-ray diffractograms of the fibrous hydrocellulose during degradation in 1.0M NaOH at 80°C.

Figure 3. X-ray diffractograms of the amorphous hydrocellulose during degradation in 1.0M NaOH at 80°C.

Figure 4. Raman spectra of the fibrous hydrocellulose during degradation in 1.0M NaOH at 80°C.

Figure 5. Raman spectra of the amorphous hydrocellulose during degradation in 1.0M NaOH at 80°C.

Figure 6. Solid-state ^{13}C-NMR spectra of the fibrous hydrocellulose during degradation in 1.0M NaOH at 80°C.

Figure 7. Solid-state ^{13}C-NMR spectra of the amorphous hydrocellulose during degradation in 1.0M NaOH at 80°C.

Figure 8. Hydrocellulose yield during degradation in 1.0M NaOH.

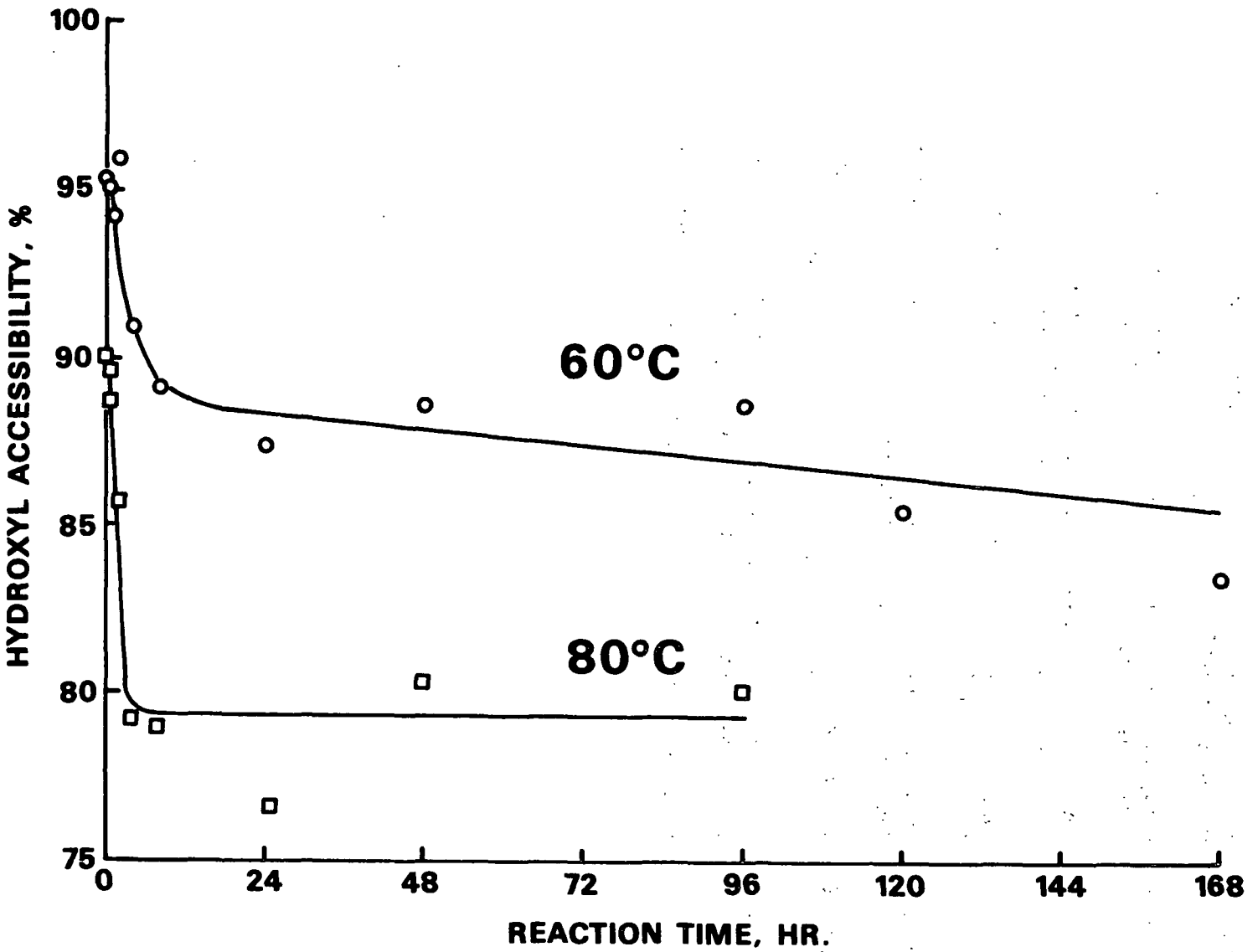

Figure 1. Hydroxyl accessibility of the amorphous hydrocellulose during degradation in 1.0M NaOH.

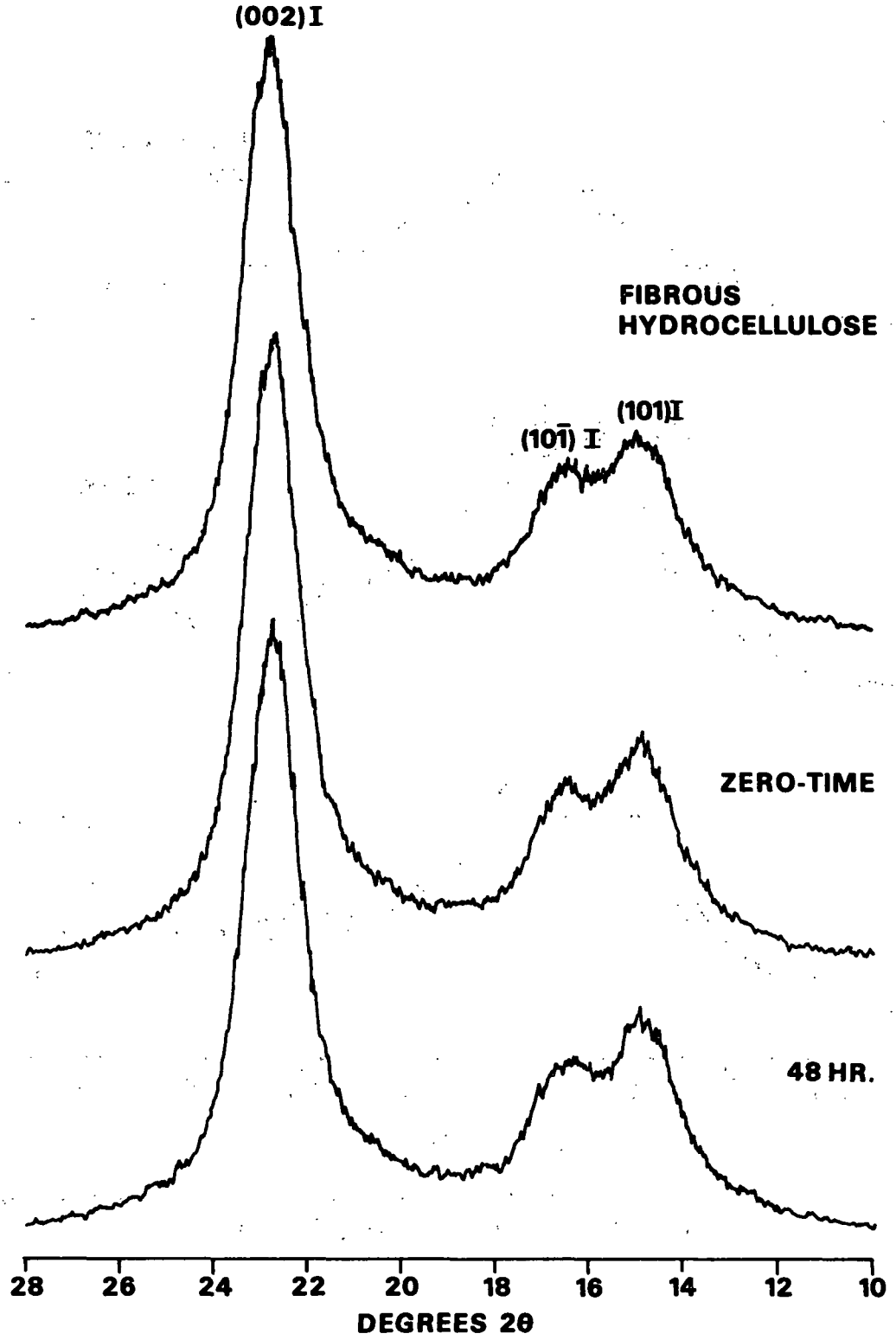

Figure 2. X-ray diffractograms of the fibrous hydrocellulose during degradation in 1.0M NaOH at 80°C.

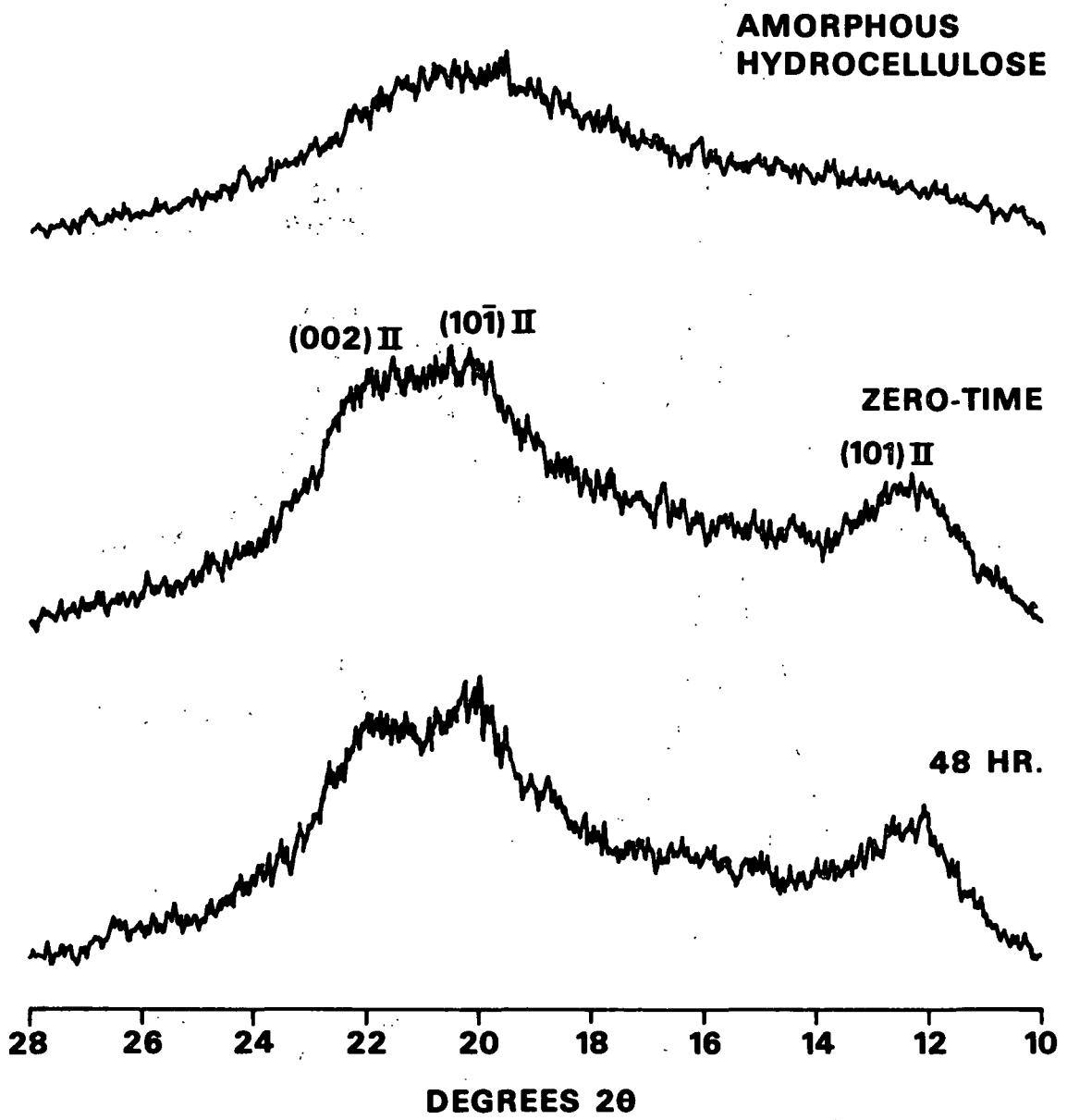

Figure 3. X-ray diffractograms of the amorphous hydrocellulose during degradation in 1.0M NaOH at 80°C.

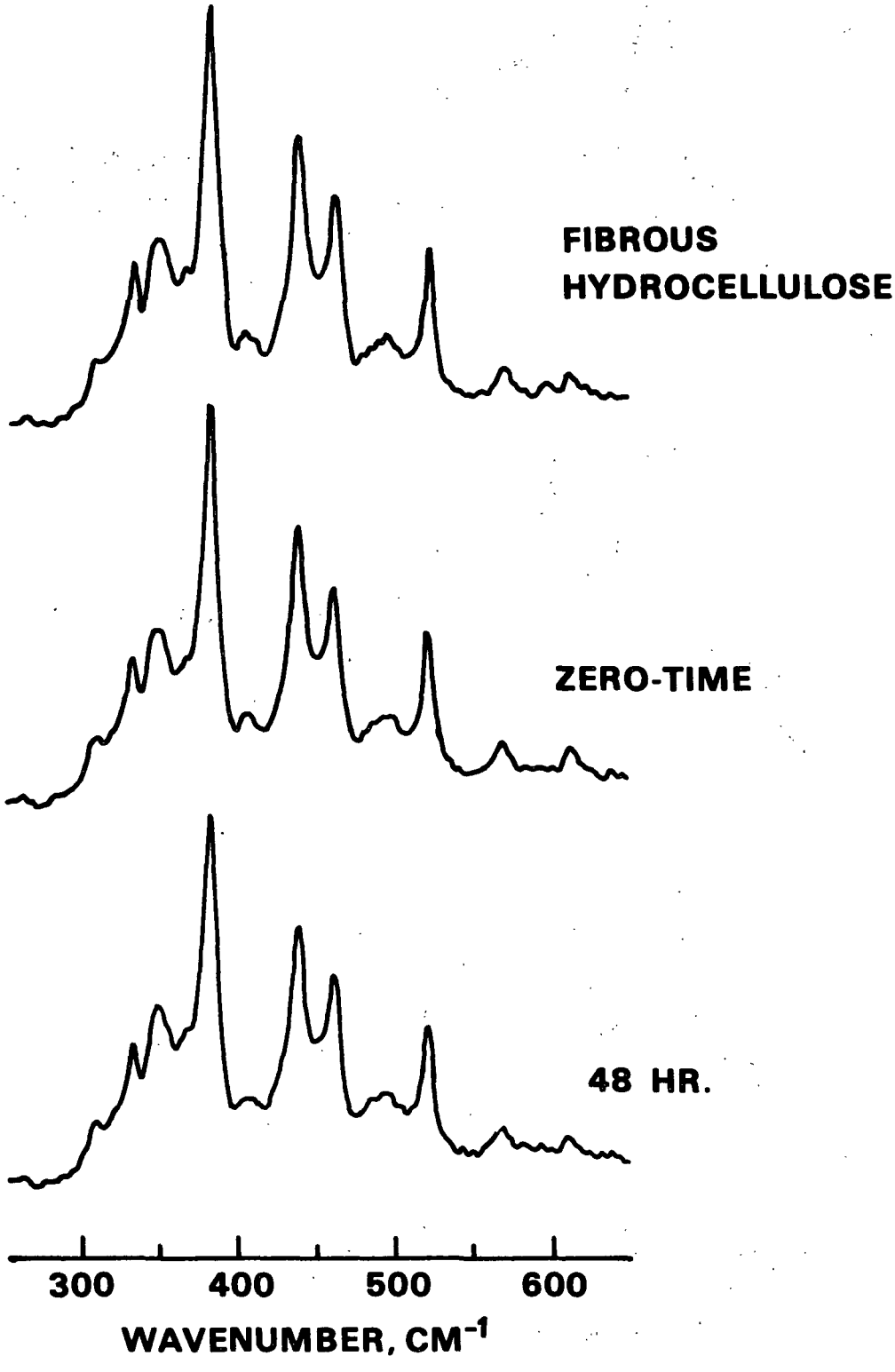

Figure 4. Raman spectra of the fibrous hydrocellulose during degradation in 1.0M NaOH at 80°C.

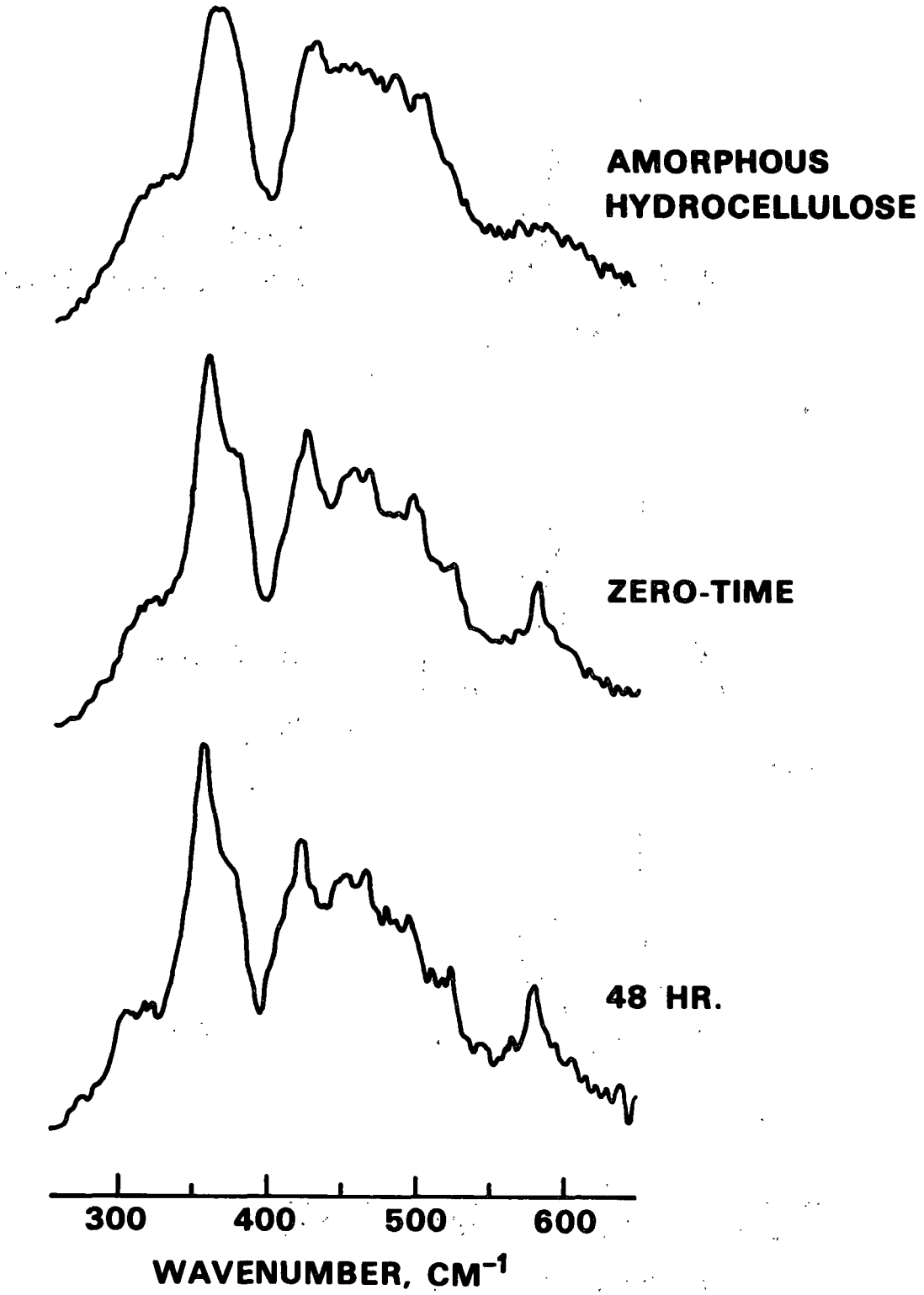

Figure 5. Raman spectra of the amorphous hydrocellulose during degradation in 1.0M NaOH at 80°C.

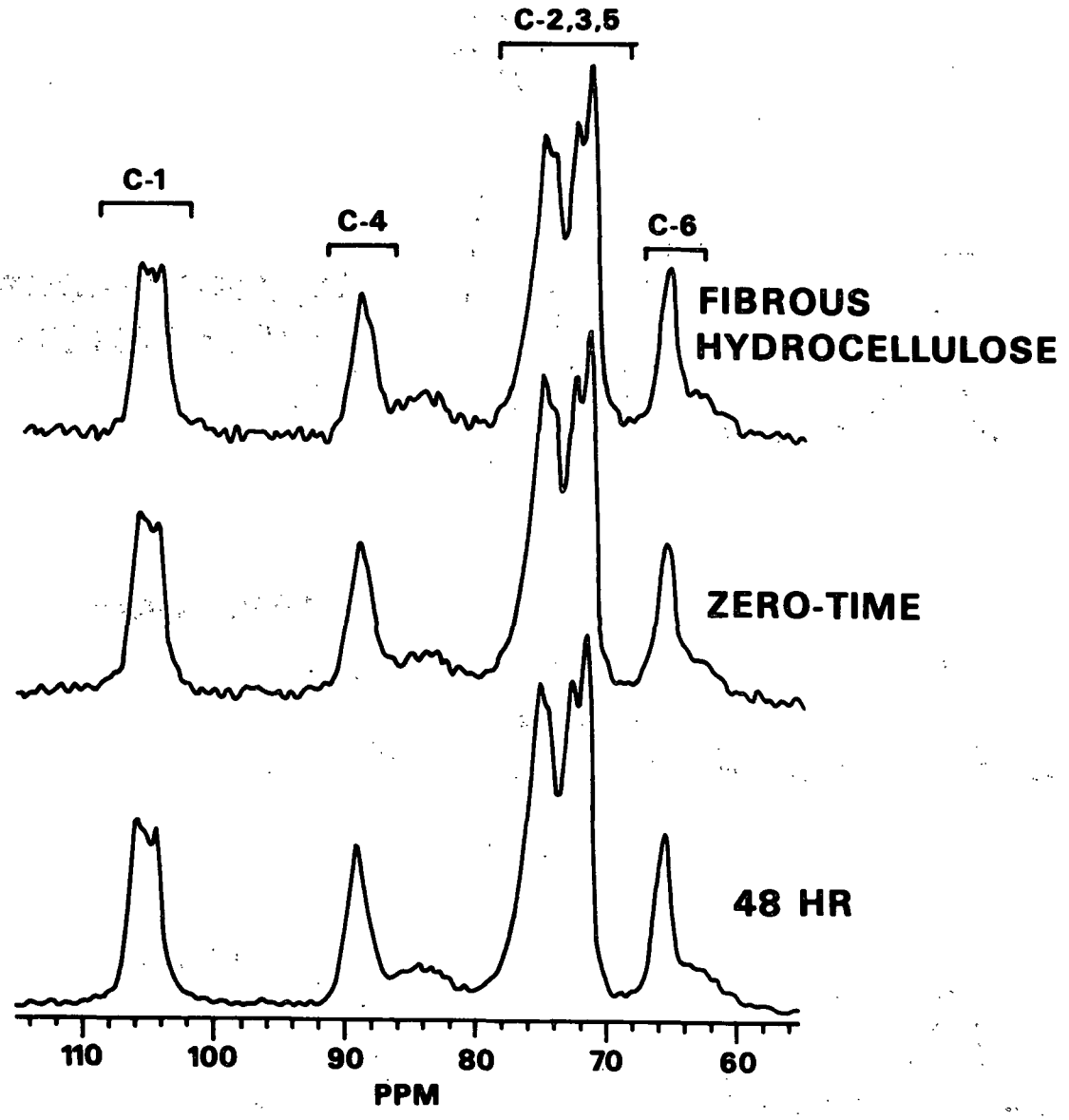

Figure 6. Solid-state ^{13}C-NMR spectra of the fibrous hydrocellulose during degradation in 1.0M NaOH at 80°C.

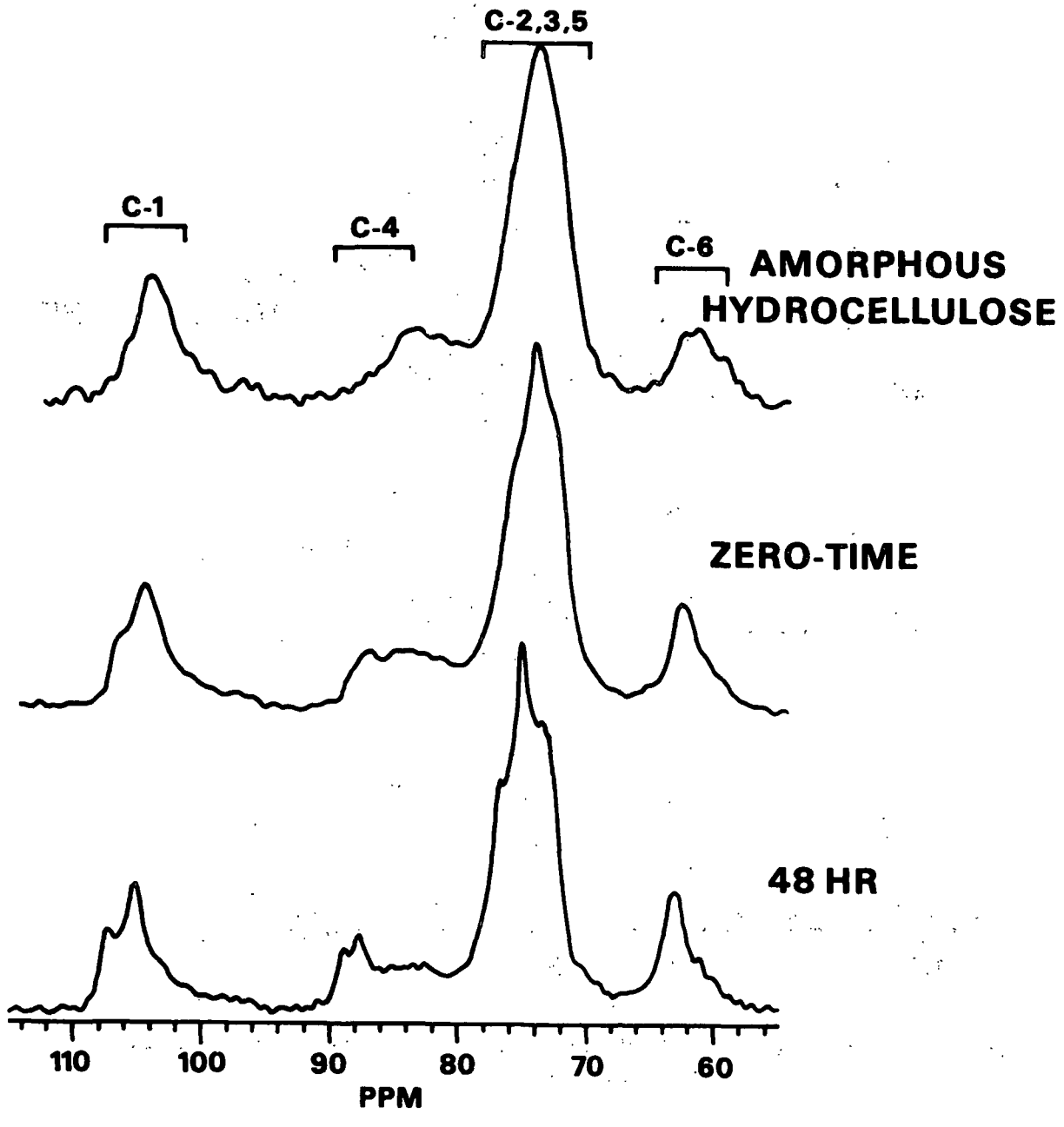

Figure 7. Solid-state ^{13}C-NMR spectra of the amorphous hydrocellulose during degradation in 1.0M NaOH at 80°C.

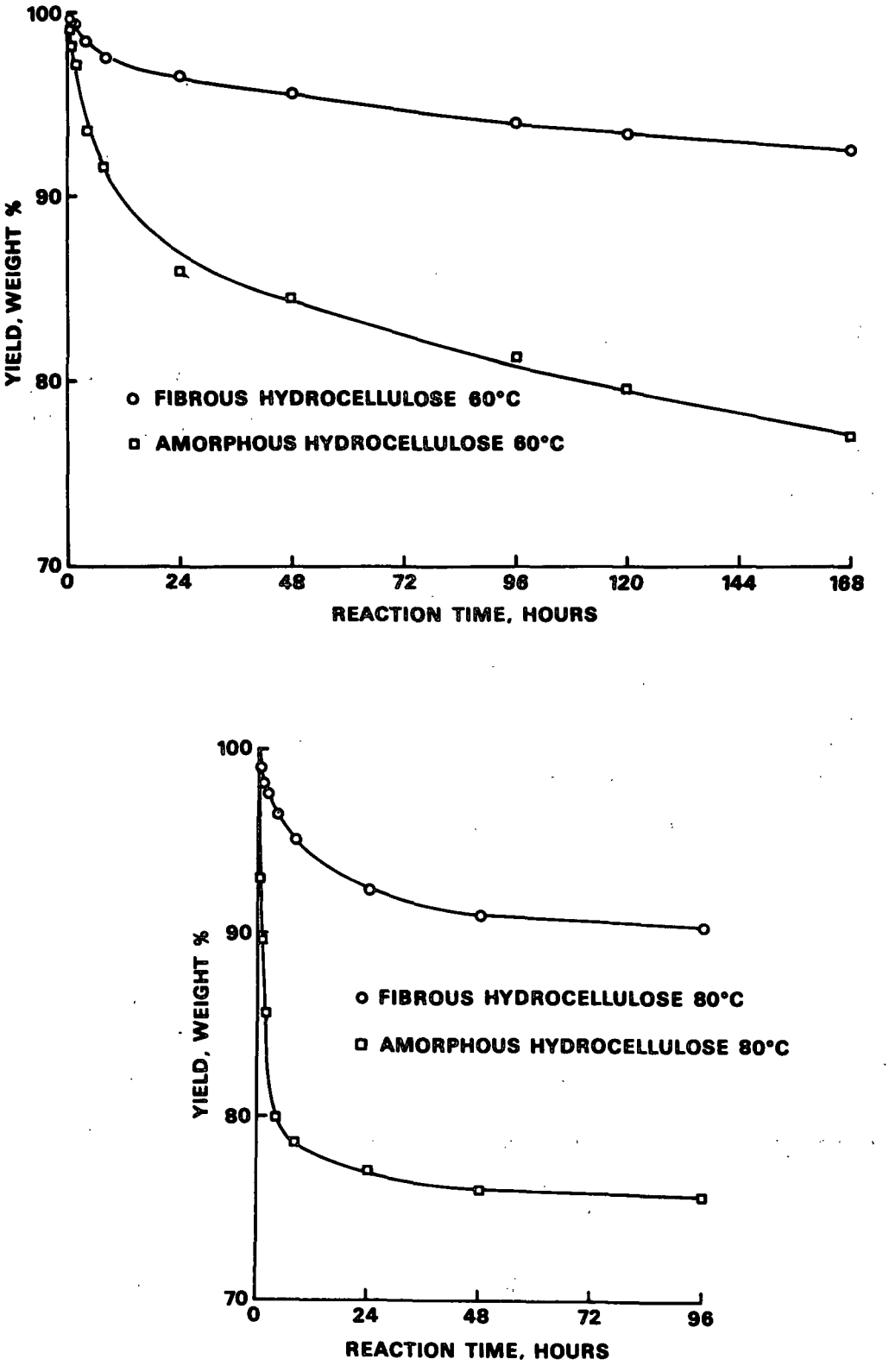

Figure 8. Hydrocellulose yield during degradation in 1.0M NaOH.